

JAERI-M
6 8 2 4

ACCURACY ANALYSIS OF THE THERMAL
DIFFUSIVITY MEASUREMENT OF MOLTEN SALTS
BY STEPWISE HEATING METHOD

November, 1976

Yoshio KATO and Kazuo FURUKAWA

この報告書は、日本原子力研究所が **JAERI-M** レポートとして、不定期に刊行している研究報告書です。入手、複製などのお問い合わせは、日本原子力研究所技術情報部（茨城県那珂郡東海村）あて、お申しこしください。

JAERI-M reports, issued irregularly, describe the results of research works carried out in JAERI. Inquiries about the availability of reports and their reproduction should be addressed to Division of Technical Information, Japan Atomic Energy Research Institute, Tokai-mura, Naka-gun, Ibaraki-ken, Japan.

Accuracy Analysis of the Thermal Diffusivity
Measurement of Molten Salts by Stepwise Heating
Method

Yoshio KATO and Kazuo FURUKAWA

Division of Nuclear Fuel Research, Tokai, JAERI

(Received November 16, 1976)

The stepwise heating method for measuring thermal diffusivity of molten salts is based on the electrical heating of a thin metal plate as a plane heat source in the molten salt. In this method, the following estimations on error are of importance : (1) thickness effect of the metal plate, (2) effective length between the plate and a temperature measuring point and (3) effect of the noise on the temperature rise signal.

In this report, a measuring apparatus is proposed and measuring conditions are suggested on the basis of error estimations.

The measurements for distilled water and glycerine were made first to test the performance ; the results agreed well with standard values. The thermal diffusivities of molten NaNO_3 at 320-380°C and of molten Li_2BeF_4 at 470-700°C were measured.

ステップ関数状加熱法による熔融塩熱拡散率測定法の精度解析

日本原子力研究所東海研究所燃料工学部

加藤 義夫・古川 和男

(1976年11月16日受理)

熔融塩の熱拡散率測定に適したステップ関数状加熱法の実用化を進めるため、装置誤差の検討を行い、誤差の推定およびその低減方法を明らかにした。

装置誤差として特に問題となるのは、(1)加熱平板(平面加熱源)の厚みの影響、(2)加熱平板と測温点間の距離、(3)測温系の信号対雑音比(S/N)などである。これらの解析にもずき、熱拡散率測定装置を試作し、標準試料とされている蒸留水およびグリセリンを測定した結果、標準データと良い一致を示した。

NaNO_3 (320–380°C)、 Li_2BeF_4 (470–700°C)等の熔融塩に対する測定結果についても述べる。

目 次 な し

I INTRODUCTION

As transient methods which measure the thermal conductivity or the thermal diffusivity of molten salts, following methods have been tried: (1) a hot wire method and (2) a plane heat source method. Others are now under developed. In these transient methods thermal diffusivity is normally obtained.

The method (1) is able to measure the thermal conductivity directly, but is not generally applicable to electrically conducting liquids which include many of the molten salts. In the method (2), a thermal diffusivity is generally measured directly except special cases.

The structure of an apparatus of the plane heat source method is not so simple as the hot wire method and it usually takes longer time to make uniform temperature distribution in the molten salt because of the larger volume of the salt in a cell. However, the plane heat source method is more suitable to measure molten salts compared with the hot wire method because of the current leakage to the salt is less and not so serious problem^{(1), (2)}.

In order to measure the thermal diffusivity of high temperature molten salt, a simple method using a plane heat source, so call stepwise heating method, was proposed in our another report⁽³⁾.

The principle of this method is as follows ; when the thin metal plate is heated stepwise in the molten salt, the ratio of the temperature rises at time t_1 and $2t_1$ at the point with distance x under the heating plate is theoretically given by the function of the Fourier number $F_0 = at_1/x^2$ where a is thermal diffusivity of the molten salt. Therefore the

thermal diffusivity α can be determined by measuring the temperature rise at the distance χ in the molten salt when the thin metal plate is heated stepwise.

The apparatus should be designed carefully to satisfy the boundary conditions of the heat conduction equation as follows. The thickness of the heating plate is sufficiently thin and wide to be regarded as one dimensional system, then the heat capacity of unit area of the plate is negligibly small and the heat flux from the plate to the molten salt is also stepwise when the plate is heated stepwise. No effect of the diameter of the sheathed thermocouple at the measuring point was also considered. The distance between the surface of the heater plate and the center line of the sheathed thermocouple was taken as the effective distance. In calculating the temperature rise ratio, the effect of noise on the temperature rise signal was not considered too.

As the analysis of these effects are important for accurate measurements, the estimations of the systematic errors and its application to the design of the apparatus and to experimental procedure are considered in this report.

II THEORY AND ACCURACY ANALYSIS

II -1 Transient Temperature Distribution Due to Stepwise Heating.

An infinite metal plate with thickness $2R$ is placed in a molten salt as shown in figure 1. Heat is produced at a constant rate $Q/2R$ per unit time per unit volume for $t > 0$ in the plate, where Q indicates the heat produced per unit time per unit surface area. The physical properties of the plate and the molten salt are distinguished by subscripts 1 and 2. The origin of the coordinate is placed at a center line of the plate.

In this case the fundamental equations for the transient temperature distribution for the metal plate and the molten salt are given as follows.

$$\frac{\partial \theta_1(x,t)}{\partial t} = a_1 \frac{\partial^2 \theta_1(x,t)}{\partial x^2} - \frac{Q}{2C_1 \rho_1 R} \quad t > 0 : -R < x < R \quad (1)$$

$$\frac{\partial \theta_2(x,t)}{\partial t} = a_2 \frac{\partial^2 \theta_2(x,t)}{\partial x^2} \quad t > 0 : R < x < \infty \quad (2)$$

Initial and boundary conditions are

$$\theta_1(x,0) = 0, \quad \theta_2(x,0) = 0 \quad (3)$$

$$\frac{\partial \theta_1(0,t)}{\partial x} = 0, \quad \frac{\partial \theta_2(\pm\infty,t)}{\partial x} = 0 \quad (4)$$

$$\pm K_\lambda \frac{\partial \theta_1(\pm R,t)}{\partial x} = \pm \frac{\partial \theta_2(\pm R,t)}{\partial x} \quad (5)$$

$$\theta_1(\pm R,t) = \theta_2(\pm R,t) \quad (6)$$

where $K_\lambda = \lambda_1/\lambda_2$.

Using Laplace transformation, the solution of eq.(1) and (2) with above initial and boundary conditions are obtained as follows.

$$\theta_1(x,t) = \frac{Q}{2RC_{p1}\rho_1} \left[1 - \frac{1}{1+K_E} \sum_{n=1}^{\infty} (-H)^{n-1} \left\{ i^2 \operatorname{erfc} \left(\frac{(2n-1)R-x}{2\sqrt{a_1 t}} \right) + i^2 \operatorname{erfc} \left(\frac{(2n-1)R+x}{2\sqrt{a_1 t}} \right) \right\} \right],$$

$$t > 0, -R < x < +R, \quad (7)$$

$$\theta_2(x,t) = \frac{2K_E Q t}{(1+K_E) C_{p1} \rho_1 R} \times \left[i^2 \operatorname{erfc} \left(\frac{x-R}{2\sqrt{a_2 t}} \right) - (1+H) \sum_{n=1}^{\infty} (-H)^{n-1} i^2 \operatorname{erfc} \left(\frac{(2n \cdot K_a^{-1/2} - 1)R+x}{2\sqrt{a_2 t}} \right) \right],$$

$$(8)$$

where $H = (1-K_E)/(1+K_E)$, $K_E = (\lambda_1 C_{p1} \rho_1 / \lambda_2 C_{p2} \rho_2)^{1/2}$, $K_a = a_1/a_2$

and $i^2 \operatorname{erfc}(y) = (1/4) [(1+2y^2) \operatorname{erfc}(y) - (2y/\sqrt{\pi}) \exp(-y^2)]$.

When $R \rightarrow 0$ in eq.(8) the limit is given as

$$\lim_{R \rightarrow 0} \theta_2(x,t) = \frac{Qx}{2\lambda} \left\{ 2\sqrt{\frac{F_0}{\pi}} \exp\left(-\frac{1}{4F_0}\right) - \operatorname{erfc}\left(\frac{1}{2\sqrt{F_0}}\right) \right\}, \quad (9)$$

where $F_0 = a_2 t / x^2$.

Equation (9) corresponds to the solution with the conditions of that the heat flux from the plate to the liquid is constantly $Q/2$ for $t > 0$.

In the case of Ni plate ($2R=0.1\text{mm}$) and $\text{H}_2\text{O}(20^\circ\text{C})$ system the temperature distributions with parameter $t(\text{sec})$ given by eqs.(7) and (8) are shown in figure 2 where $Q = 2\text{W/cm}^2$. In this figure the temperature difference $\Delta\theta$ between the surface of the plate and the measuring point should be noted. For example, when the temperature at the point $x/R=40$ is about 0.5°C on the curve of 4 sec, the temperature at the plate surface is about 14°C , then the difference is about 13.5°C .

However, if Q is reduced to $1/10$ (0.2W/cm) the unit of the temperature axis should be reduced to $1/10$ because the θ_2 is linearly proportional to Q in eq.(8). For molten salts which have the thermal properties with large temperature dependence, $\Delta\theta$ should be small. In such a case Q should be taken small and measuring time should be taken relatively long.

According to a numerical analysis, the temperature difference $\Delta\theta$ does not so much depend on the thickness of the plate in the case of $2R < 0.5\text{mm}$.

The heat flux from the plate is given as

$$q = -\lambda_2(\partial\theta_2/\partial x)_R. \quad (10)$$

The result of above calculation using eq.(8) is shown in figure 3 where the parameter is plate thickness and physical properties of Ni plate and of H_2O (20°C) are used. From the figure 3, it is noted that if $2R < 0.02\text{mm}$, the time to reach 99% of saturated heat flux is less than about 0.8sec, and well approximate stepwise heat flux can be obtained.

II -2 The Theoretical Analysis on The Ratio of Temperature Rises vs. Fourier Number

Using eq.(8), the ratio of temperature rises at time t_1 and $2t_1$ is given as a following equation which is a function of F_0 and is also characterised by three parameters H , K_a and X_R .

$$\frac{\theta_2(x, 2t_1)}{\theta_2(x, t_1)} = \frac{2\{i^2 \text{erfc}(1/2\sqrt{2F_0}) - (1+H) \sum_{n=1}^{\infty} (-H)^{n-1} i^2 \text{erfc}[(2n \cdot K_a^{1/2} X_R^{-1} + 1)/2\sqrt{2F_0}]\}}{i^2 \text{erfc}(1/\sqrt{2F_0}) - (1+H) \sum_{n=1}^{\infty} (-H)^{n-1} i^2 \text{erfc}[(2n \cdot K_a^{1/2} X_R^{-1} + 1)/2\sqrt{F_0}]},$$

where $F_0 = \alpha_2 t_1 / X^2$, $X_R = X/R$ and $X = x - R$.

Also, the ratio of temperature rises in the case of $R=0$ is given by eq.(9) as follow.

$$\frac{\theta_2(x, 2t_1)}{\theta_2(x, t_1)} = \frac{2(2F_0/\pi)^{1/2} \exp(-1/8F_0) - \operatorname{erfc}(1/2(2F_0)^{1/2})}{2(F_0/\pi)^{1/2} \exp(-1/4F_0) - \operatorname{erfc}(1/2F_0^{1/2})}, \quad (12)$$

where $F_0 = a_2 t_1 / x^2$.

It could be generally assumed for molten salts that $K_g > 1$, then the theoretical curves given by eq. (11) would exist in the region between the curves of $R=0$ and of $H=-1$ as shown in figure 4. For the system of $H_2O(20^\circ C)$ and Ni plate ($2R=0.1mm$), the curve is also shown in figure 4.

The dependence of the eq. (11) on these parameters should be estimated. Figure 5 shows that the dependence of eq. (11) on H with $K = 100$, $X = 50$. Also figures 6 and 7 show the dependence on X with $H = -0.85$, $K_a = 100$ and the dependence on K_a with $H = -0.85$, $X = 50$. The curves shown in these figures approach to the curve of $R=0$ with decrease of $|H|$ and with increase of K_a and X_R .

If the material of the heater plate is determined, X_R is only variable in these parameters. The value of X_R should be chosen to a optimum value to get adequate ratio of temperature rises ⁽³⁾.

In many cases the physical properties λ_2 , C_{p2} and ρ_2 of the molten salts are not accurately known, therefore the parameters H and K_a are not obtained. However if C_{p2} and ρ_2 are already known together with the values of C_{p1} , ρ_1 and λ_1 it is able to determine the approximate values of H and K_a by using the value Q_2^0 which is obtained by a preparatory measurements assuming $R=0$.

If the values of λ_2 , C_{p2} and ρ_2 are unknown, a_2 have to be determined approximately by eq. (12) assuming $R=0$. In this case the error caused by using eq. (12) could be evaluated as follows with the assumed value of H .

If the errors of time t_1 and distance X in the Fourier number could be neglected, the error of α_2 is obtained as follows.

$$\frac{\Delta \alpha_2^H}{\alpha_2^H} = \frac{\Delta F_0^H}{F_0^H},$$

where α_2^H and F_0^H are the values obtained from eq.(11) assuming a value of H , α_2^0 and F_0^0 are the values obtained from eq.(12) for the same ratio of the temperatures.

Figure 8a and 8b show that the relation between the error and the parameter H with several X_R ($K_A=50, 100$) and with several K_A ($X_R=30$).

Figure 9a and 9b show that the relation between the error and the parameter X_R with several H ($K_A=50, 100$) and with several K_A ($H=-0.85$).

Also figure 10a and 10b show that the relation between the error and the parameter K_A with several X_R ($H=-0.85, -0.80$) and with several H ($X_R=30$).

These relations are taken for $\theta(x, 2t_1)/\theta(x, t_1)=3$. If the ratio of the temperature rises are taken to the value more than 3, these errors shown in these figures are all decrease slightly as shown in figure 11.

To make the error less than +5% without correcting these parameters effect, X_R should be taken more than 100 in ordinary case of $K_A > 50$ and $H > -0.9$.

The effect of H increase extremely in the region $0.95 < |H| < 1.0$. However, figure 12 shows that the value $|H|$ may be less than 0.9 and more than 0.4 for many molten salts. The value of $|H|$ decreases by using a platinum heater plate instead of nickel plate. Then it is more practical in the error estimation that H is assumed to exist in the region $-0.4 > H > -0.9$.

For example, if the value of H is assumed to -0.80 as a suitable value, the error calculated by eq.(11) is about $+3.5\%$ for $H=-0.9$ (assumed maximum) and about -2.6% for $H=-0.4$ (assumed minimum), then the error about $\pm 3.5\%$ is secured as long as $-0.4 > H > -0.9$.

II-3 The Effect of Finite Heater Plate

To simplify the problem, the width of the heater plate is assumed to be finite in the previous section. The practical width should be determined by considering the horizontal boundary effect. It is easy to evaluate the effect experimentally by measuring the thermal diffusivities of a sample liquid at several points keeping parallel to the heater plate. The result is shown in figure 13. It is the case of $32 \times 32 \times 0.1$ mm heater plate (Ni alloy) and distilled water (20°C). Under the region of 7.5 mm from the center of the plate, end effect may be neglected in this case.

II-4 The Method to Determine The Effective Distance l_{eff} .

When the thermal diffusivity α_2 is determined from the Fourier number, the estimation of effective distance l_{eff} between the heater plate and the measuring point is another important problem. There are two problems to determine the l_{eff} .

The first is how to detect the zero point of l_{eff} . The change of the distance from a reference point, Δl , can be measured within a reading error of about $1/100 \sim 1/500$ mm by using micrometer or electrical differential transformer. However for some kinds of molten salts, it is difficult to detect the contact

point(zero point) of the sheathed thermocouple and the heater plate by optical or by electrical method.

The second is how to evaluate the effective temperature detection point on a diameter of the sheathed thermocouple because the diameter, even if 0.25mm, is not negligible to the distance l_{eff} of about 1~2 mm.

For these problems following method is usefull to determine the l_{eff} . When the heater plate is heated stepwise at a constant rate, the temperature rise of the sample salt should be measured at several point of vertical direction under the heating plate. From each trace of temperature rise curves, the transient temperature distribution of the sample liquid is obtained with parameter $t(\text{sec})$ as shown in figure 14. The temperature of the heater plate itself should be also measured.

From the cross point of the two temperature curves of the sample liquid and the heater plate, the origin (zero point) is determined. Then the effective distance l_{eff} is obtained by the difference between the measuring point and the zero point indicated on the micrometer. The second problem mentiond above is solved at the same time in this method.

II-5 The Effect of Noise Component on The Temperature Rise Curve.

Data recording and processing systems are shown in figure 15. The thermoelectromotive force of the sheathed thermocouple[1] is amplified by D.C. amplifier[2]. The noise component of the out put signal is filtered out by low pass filter[3] and the signal is recorded by digital recorder[4](10bit 1K word). The

recorded data are monitored by oscilloscope [5] and punched out by paper tape puncher[6]. The data of the punched paper tape are processed by a computer[7].

Noise component of the temperature rise signal affects largely to the accuracy of temperature rise ratio. If $\theta(x, 2t_1)$ is taken to about 1°C (about $40\mu\text{V}$ by Chromel-Alumel thermocouple) and the temperature rise ratio is taken to about 4, the error of the ratio reaches to about 30% because the total noise component of the thermocouple and the D.C. amplifier(input noise) is constantly about $2\mu\text{V}_{\text{rms}}$.

To reject the noise component, low pass filter(42db/oct decrease from a cutoff frequency) and 50Hz (power source noise) rejection filter are used. If the cutoff frequency of the low pass filter is lowered from 50Hz to decrease the noise level, the effect of the signal (wave form) distortion increases. The effect of the cutoff frequency of the low pass filter is shown in figure 16. To decrease the noise level in low frequency region without wave form distortion, numerical data smoothing is taken in computer program.

However it is difficult to reject the noise component sufficiently and to make the error of temperature rise ratio within about $\pm 2\%$.

To solve this problem, many times t_1 should be selected appropriately and many temperature rise ratios should be obtained from one temperature rise curve. Then the mean thermal diffusivity can be determined from these data.

Usually the times t_1 are taken to about 100 to 200 points every 10m second.

III IMPROVED APPARATUS AND PROCEDURE

An apparatus shown in figure 17 is designed as the results of the above analysis considering the experiences of the previous apparatus⁽³⁾. Improved points are as follows.

- (1) The position of the thermocouple for temperature rise measurement is possible to regulate from outside of the cell keeping gas tight. An electrical zero point detector is equipped and a micrometer is used for positioning of the thermocouple.
- (2) The heating plate is made of nickel alloy of 0.1mm thick (32 X 32mm width) and is exchangeable.
- (3) Inconel sheathed Chromel-Alumel thermocouple of 0.25mm O.D. is used for improving the thermal response.
- (4) The position of an outer furnace heater is possible to regulate and the vertical temperature distribution in the cell is able to regulate minutely.
- (5) The electrodes of the heater plate have a shape of half cylindrical shell to prevent the sample salt from direct irradiation of inner surface of the furnace heater.

The heater plate 1 is fixed on the plate holder 2 by screws together with the Beryllia skirt 3 which avoids convection flow. The heater plate holder is also set on the half-cylindrical shell electrodes 4 by screws. The sheathed thermocouple 5 is set on the bottom of the quartz pot 6 and is able to control the position to vertical direction with the pot. The pot is set on the quartz center pillar 7 and the other side of the pillar

is connected to the micrometer 8. The position of the outer furnace heater 10 is able to shift vertically.

The radiation shield plates 9 are fixed on the guide tube of the center pillar to prevent temperature rise of lower side of the cell. The lower part of the outer quartz cell and its mount are cooled by water. The top part (about 5mm) of the sheathed thermocouple 5 is made parallel to the heater plate.

IV RESULTS

To examine the performance of this apparatus, the thermal diffusivities of distilled water and of glycerine were measured. The results were well agreed with the standard values. The results of the glycerine is shown in figure 18 together with the values converted from published data.⁽⁴⁾

From the figure 18 we can read the mean values as $(3.4 \pm 0.2) \times 10^{-4} \text{ m}^2 \text{ h}^{-1}$ at 20°C and $(2.9 \pm 0.2) \times 10^{-4} \text{ m}^2 \text{ h}^{-1}$ at 200°C. These results were obtained by using the parameters X_R , K_a and H . The mean value of $H = -0.90$ was calculated from the published data.

The thermal diffusivities of molten salts were then measured. In figure 19 the experimental results for molten NaNO_3 at 320-380°C are shown together with published data.⁽²⁾

Mean value of parameter $H = -0.85$ was used in the calculation.

No temperature dependence was observed and the mean value of $\alpha = (5.5 \pm 0.5) \times 10^{-4} \text{ m}^2 \text{ h}^{-1}$ was obtained. The difference between the measured values and the referenced one shown in figure 19 was about 7%.

The experimental results for molten Li_2BeF_4 at 470-700°C are shown in figure 20 together with values converted from published data.⁽⁵⁾

From figure 20 we can read the mean values as $(7.5 \pm 0.9) \times 10^{-4} \text{ m}^2 \text{ h}^{-1}$ at 470-700°C. Mean value of parameter $H = -0.78$ obtained from the published data of referenced one was also used in the calculation.

It is estimated that the scattering of the data depends on the initial thermal stability of the salt and on the existence of the gas babbles on the heating plate. In the case of Li_2BeF_4 , the initial rate of temperature drift was kept below $0.05^\circ\text{C min}^{-1}$.

The measurements for the molten salts were made in an argon atmosphere at a pressure about 10 Torr higher than atmospheric.

V CONCLUSION

Following conclusions are obtained.

- (1) According to the analysis on the transient temperature distribution, the temperature difference between the heater plate and the measuring point should be small for molten salts which have the thermal properties with large temperature dependence. In such a case, heat generating rate should be taken small and measuring time should be taken relatively long.
- (2) Three parameters H , K_a and X_R have to be considered at the same time to reduce the error caused by the thickness of the heater plate. When the effect of the thickness of the heater plate is corrected, the accuracy depends on the approximation of these parameters. In these parameters,

X_R can be obtained accurately and approximate value of K_a is obtained from preparatory measurement with the curve of $R=0$ but in general there are no accurate information on H . However in ordinary cases, the value of H could be assumed to $H > -0.9$, the assumed maximum error of the thermal diffusivity obtained from the curve of $R=0$ can be estimated practically in comparison with the value obtained from the curve of $H=-0.9$.

- (3) If $X_R > 100$, $K_a > 50$ and $H > -0.9$, the error of the thermal diffusivities obtained from the curve of $R=0$ is less than +5%.
- (4) Many temperature rise ratio should be taken from one temperature rise curve to avoid the error caused by the noise on the signal.

The thermal diffusivity should be determined from the average of these data.

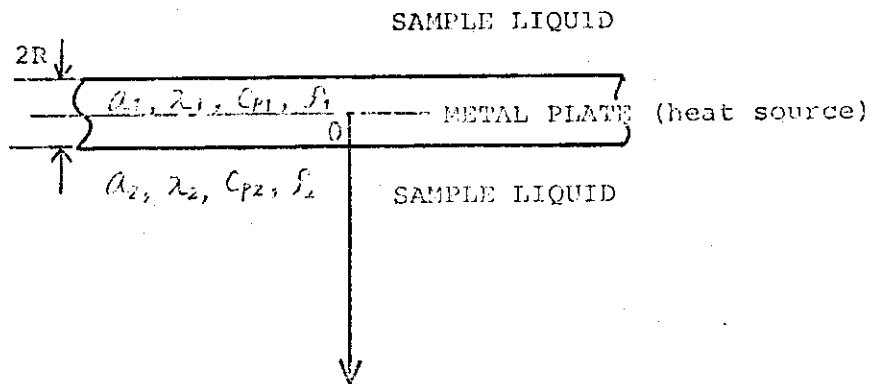
- (5) An improved apparatus has been made and its good performance was verified by measurements of distilled water and glycerine.
- (6) Measurements of molten salts were made on NaNO_3 at 320-380°C and Li_2BeF_4 at 470-700°C.

ACKNOWLEDGMENT

The author is pleased to acknowledge Prof. Kiyosi Kobayasi and Dr. Nobuyuki Araki of Shizuoka University for help with every phase of this work.

Reference

- (1) L.R.White and H.T.Davis, J.Chem.Phys.47(1967)5433-9
- (2) S.E.Gustafsson, N.O.Halling and R.A.E.Kjellander,
Z.Naturforsch. 23a, (1968)44-7
- (3) Y.Kato, K.Kobayasi, N.Araki and K.Furukawa,
J.Phys.E:Sci.Instrum. 8(1975)461-4
- (4) Y.S.Touloukian (ed): Thermophysical Properties of Matter
(New York:IFI/Plenum Data Coap)
- (5) J.W.Cooke, ORNL-4728(1972)41



α : THERMAL DIFFUSIVITY

λ : THERMAL CONDUCTIVITY

C_p : SPECIFIC HEAT AT CONSTANT PRESSURE

ρ : DENSITY

Fig. 1 Heat source of finite thickness plate.
The origin of the coordinate is placed at the center line of the plate.

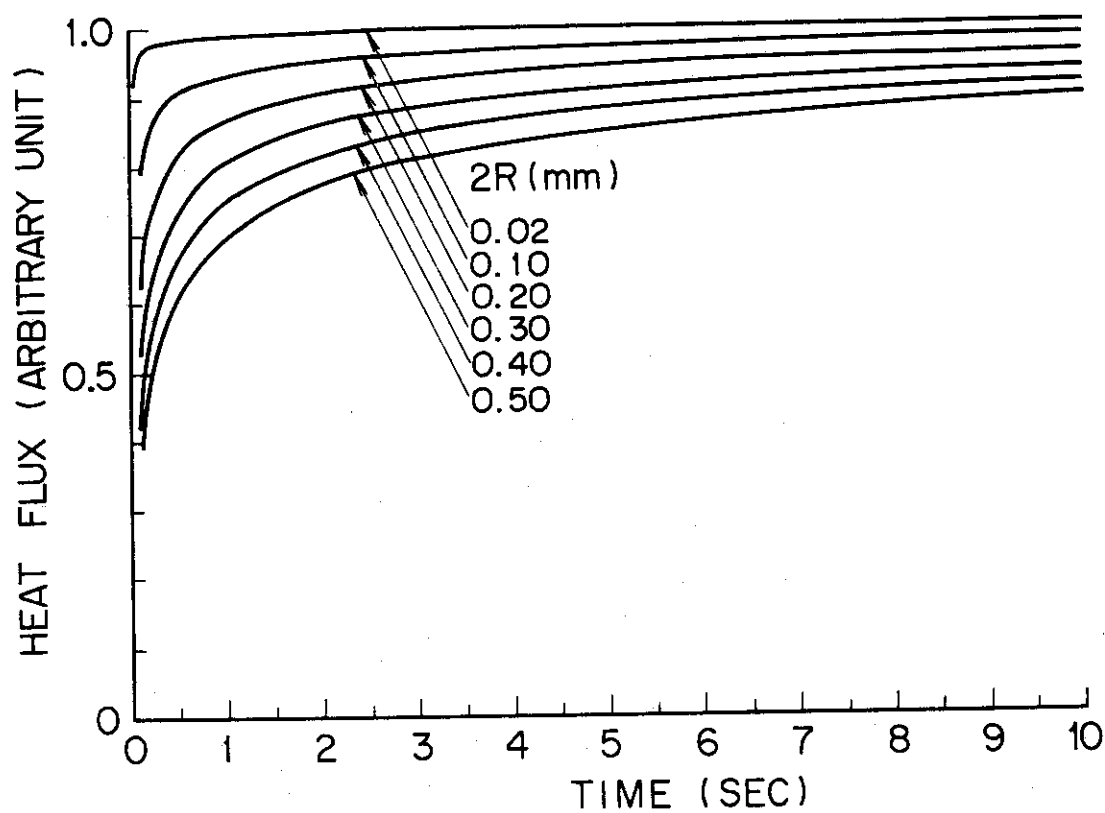


Fig. 3 Heat flux from Ni plate to $H_2O(20^\circ C)$.

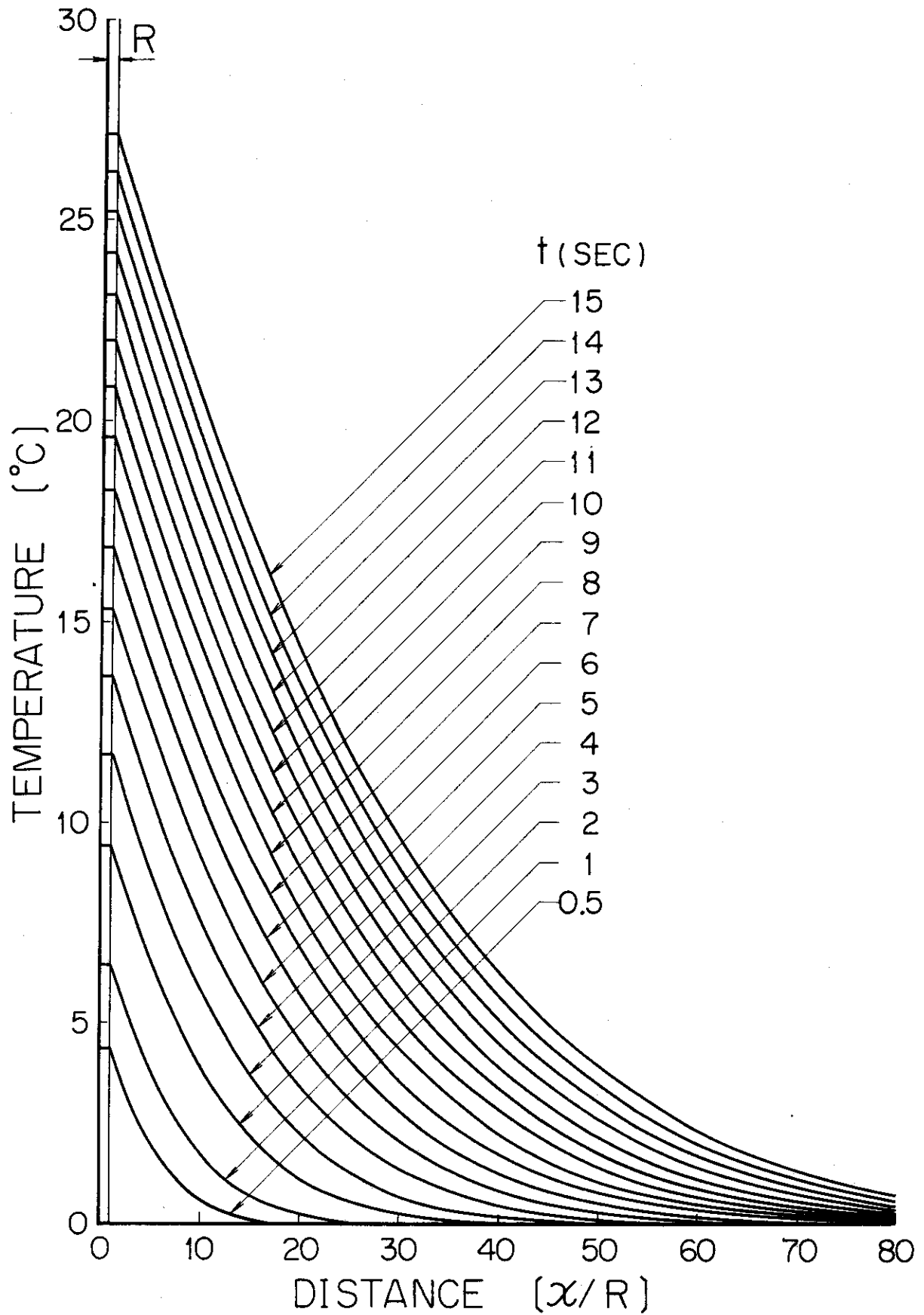


Fig. 2 Transient temperature distribution due to stepwise heating in the case of Ni plate ($2R=0.1\text{mm}$) and H_2O system. $Q=2\text{W/cm}^2$.

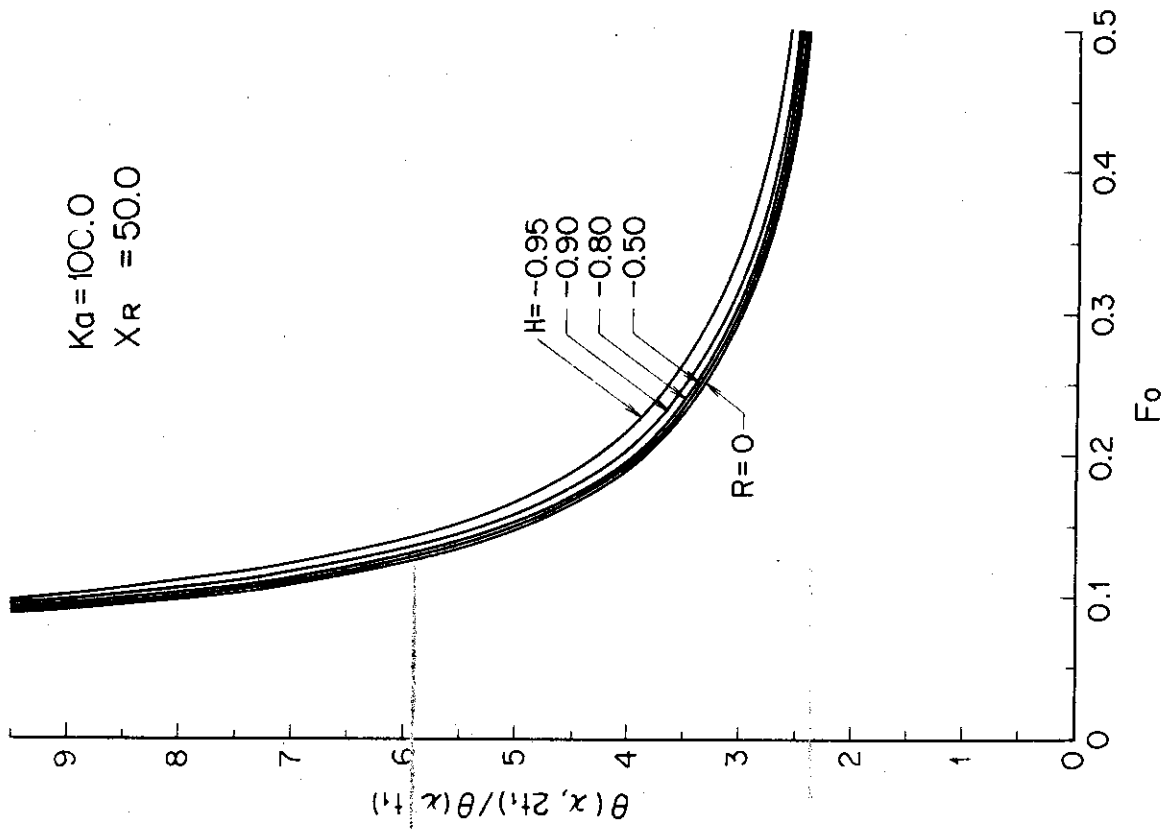


Fig. 5 Effect of the parameter H on the theoretical curve of the ratio of temperature rises ($K_a=100, X_R=50$).

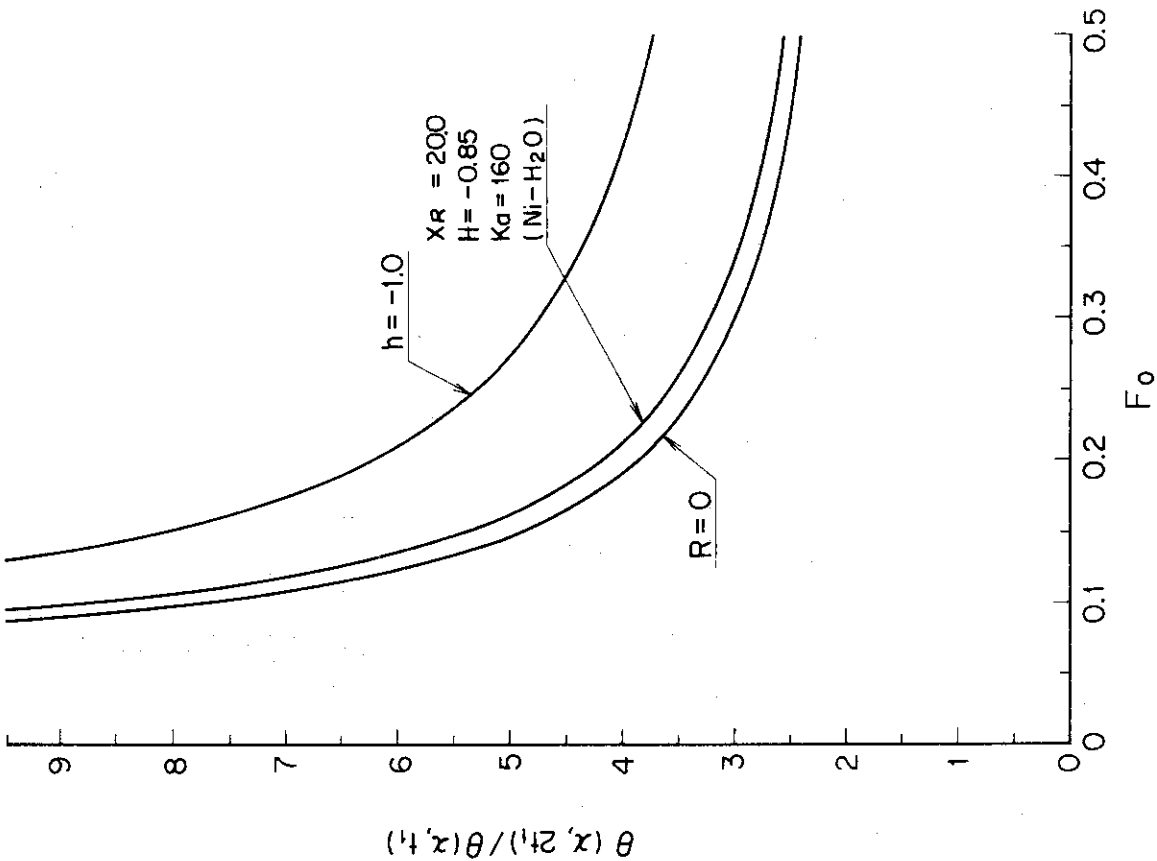


Fig. 4 Region in which theoretical curves of the ratio of temperature rises exist. The case of Ni plate- H_2O system is shown in the region.

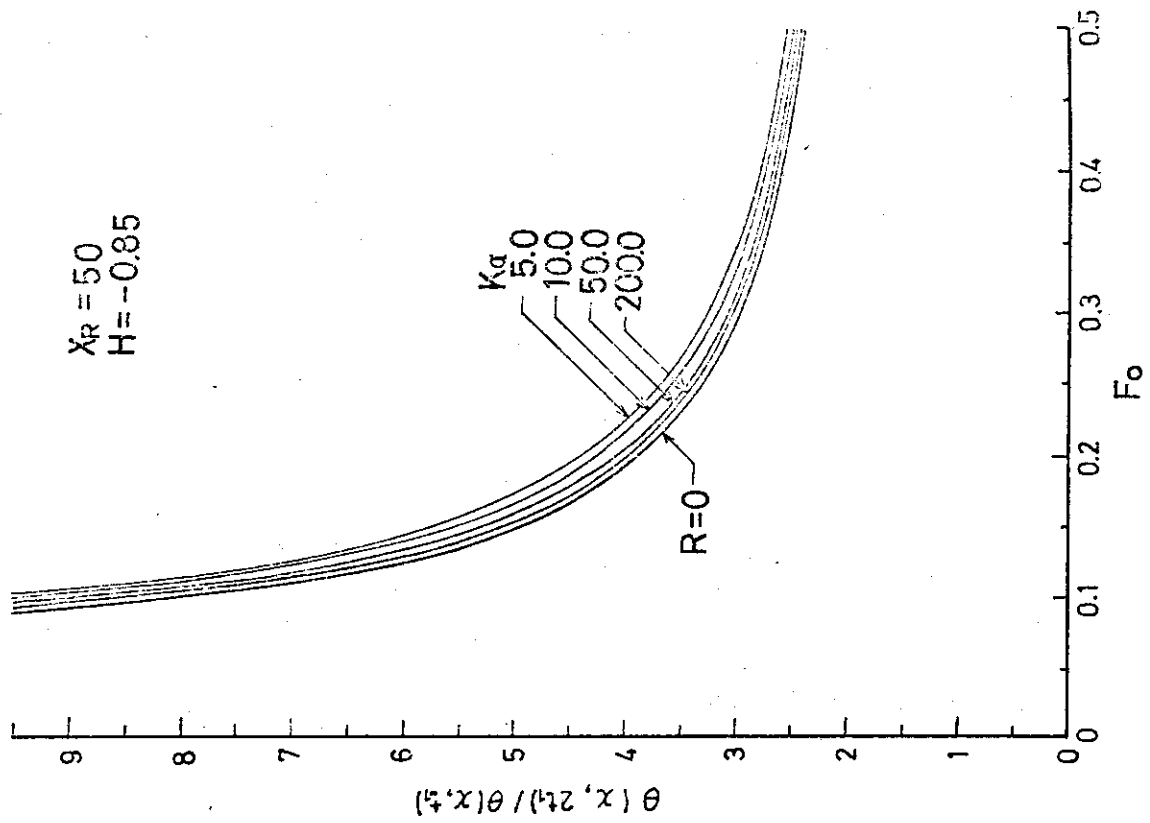


Fig. 7 Effect of the parameter Ka on the theoretical curve of the ratio of temperature rises ($X_R=50, H=-0.85$).

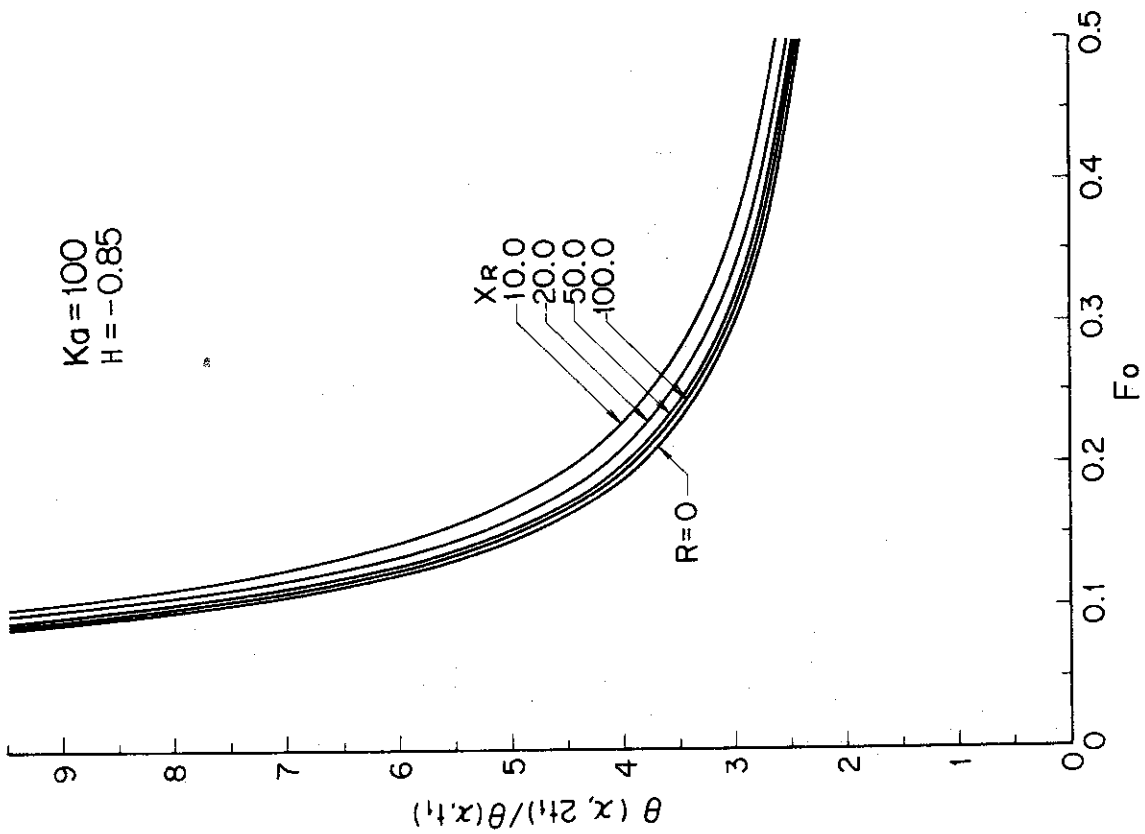


Fig. 6 Effect of the parameter X_R on the theoretical curve of the ratio of temperature rises ($H=-0.85, Ka=100$).

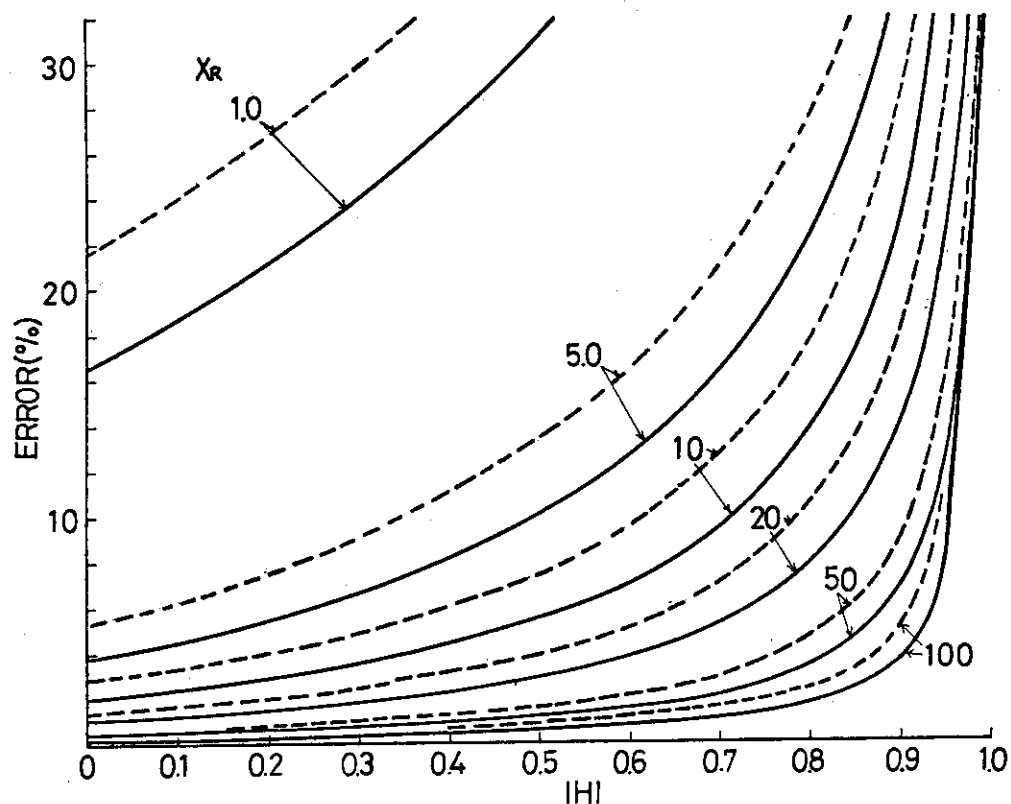


Fig. 8a Error caused by neglecting the thickness of the heater plate.
Effect of the parameter X_R on the relation of error vs. $|H|$ (temperature rise ratio=3, $K_a=50$ ---, 100—).

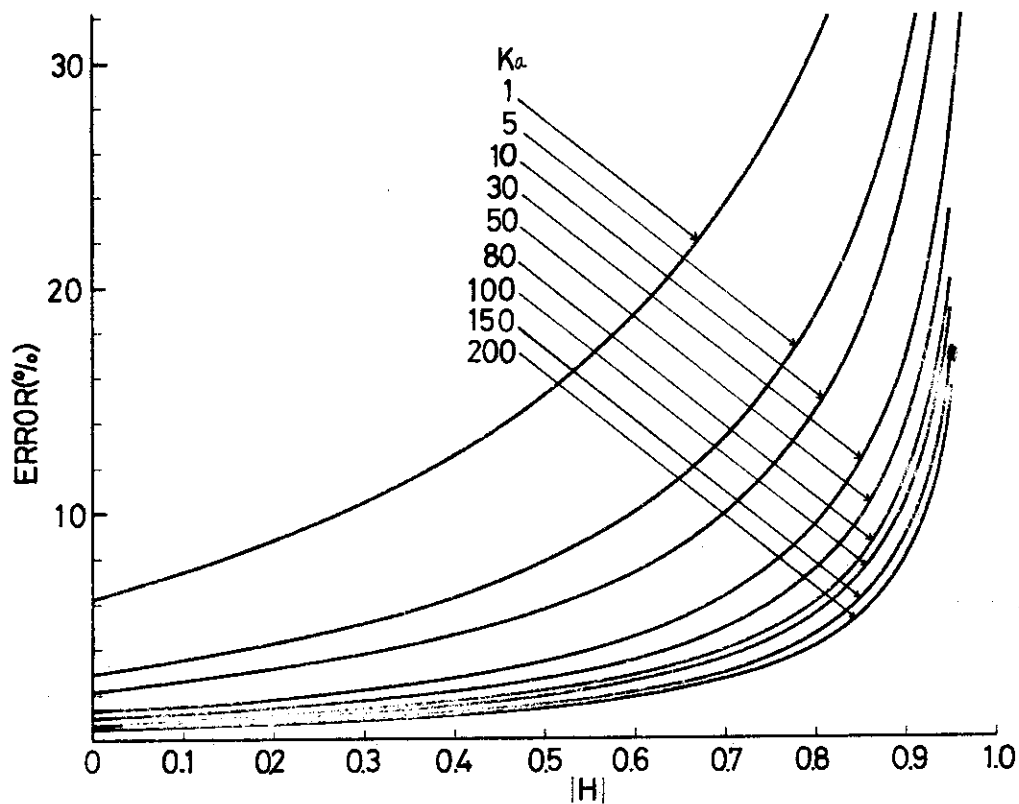


Fig. 8b Effect of the parameter K_a on the relation of error vs. $|H|$ ($X_R=30$).

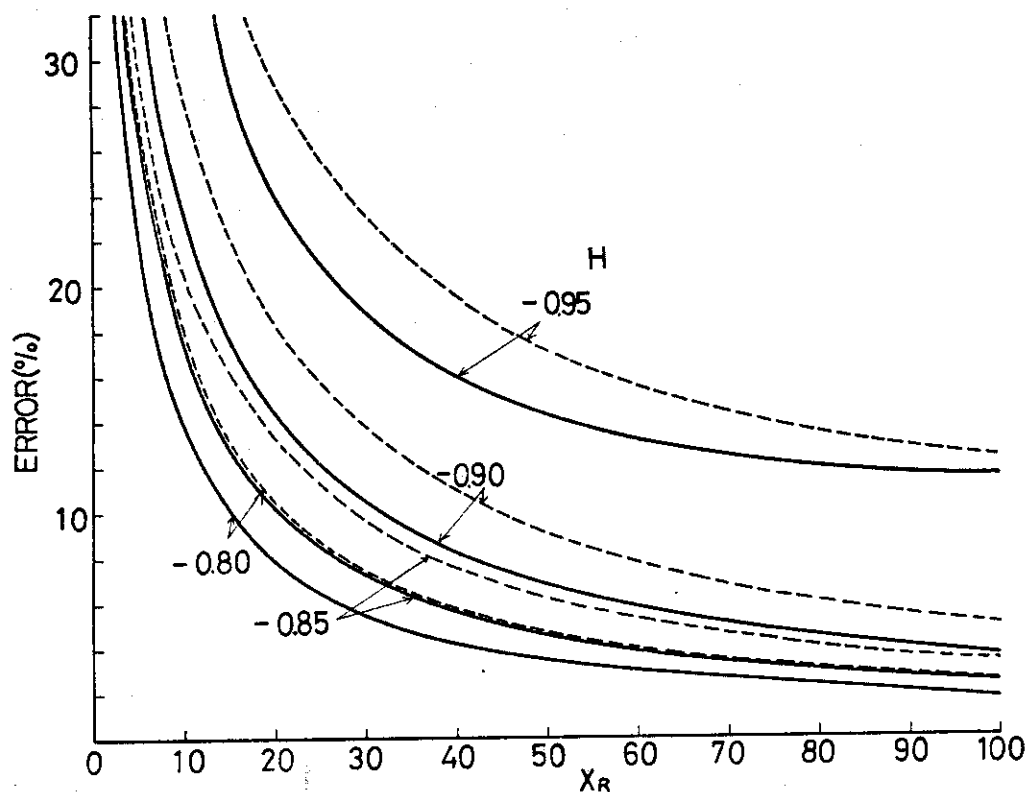


Fig. 9a Error caused by neglecting the thickness of the heater plate.
Effect of the parameter H on the relation of error vs. X_R (temperature rise ratio=3, $K_a=50$ ---, 100—).

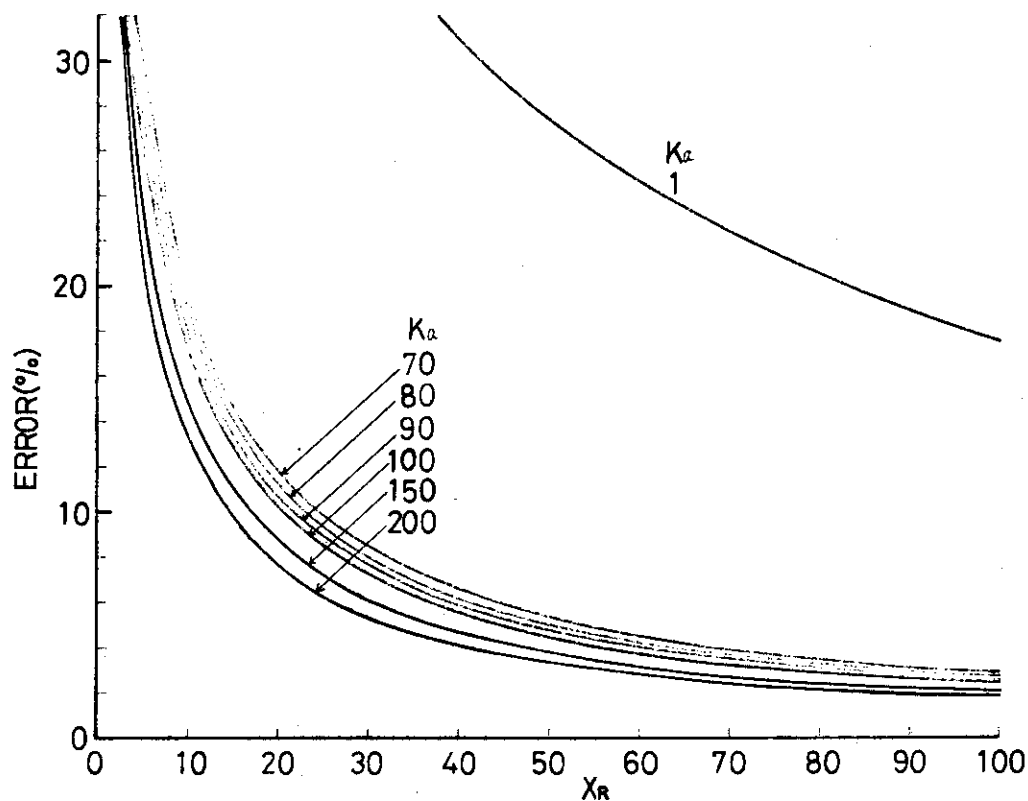


Fig. 9b Effect of the parameter K_a on the relation of error vs. X_R ($H=-0.85$).

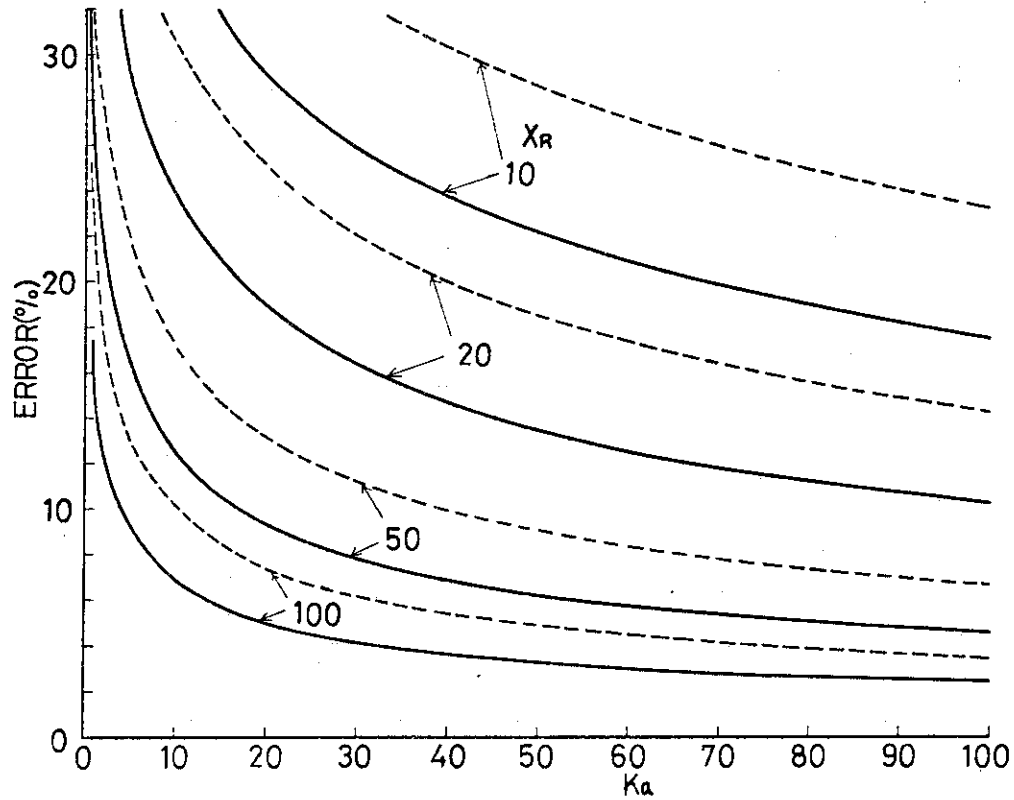


Fig. 10a Error caused by neglecting the thickness of the heater plate.
Effect of the parameter X_R on the relation of error vs. Ka (temperature rise ratio=3, $H=-0.9$ ---, -0.85 —).

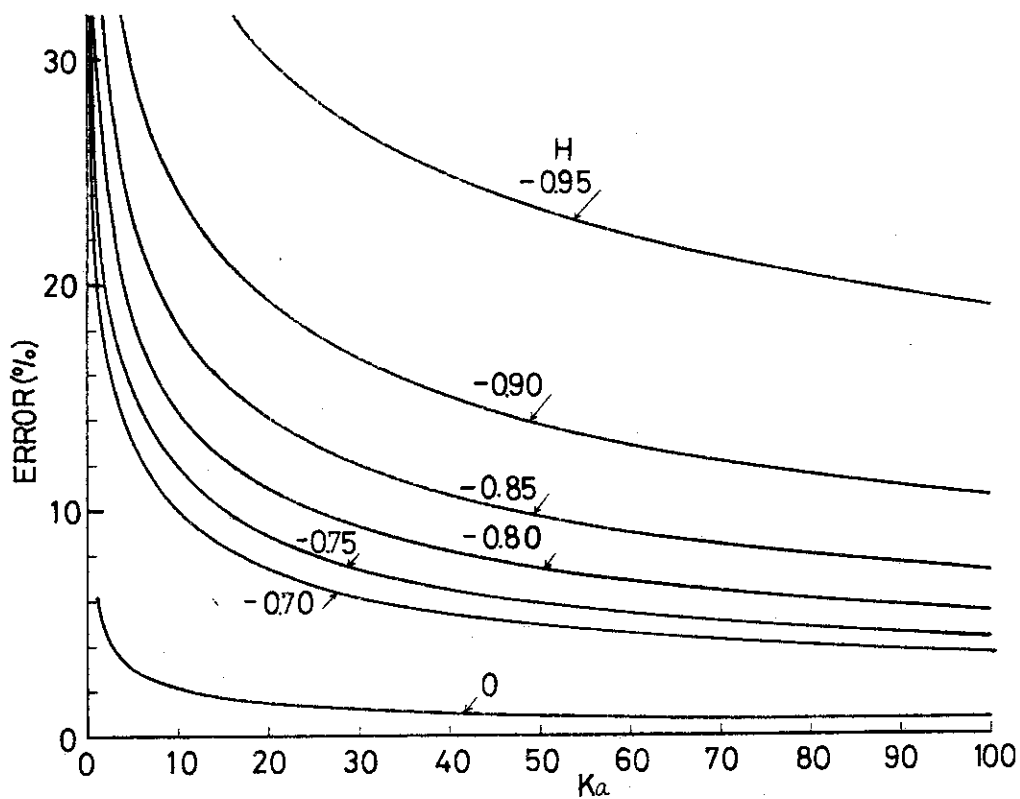


Fig. 10b Effect of the parameter H on the relation of error vs. Ka ($X_R=30$).

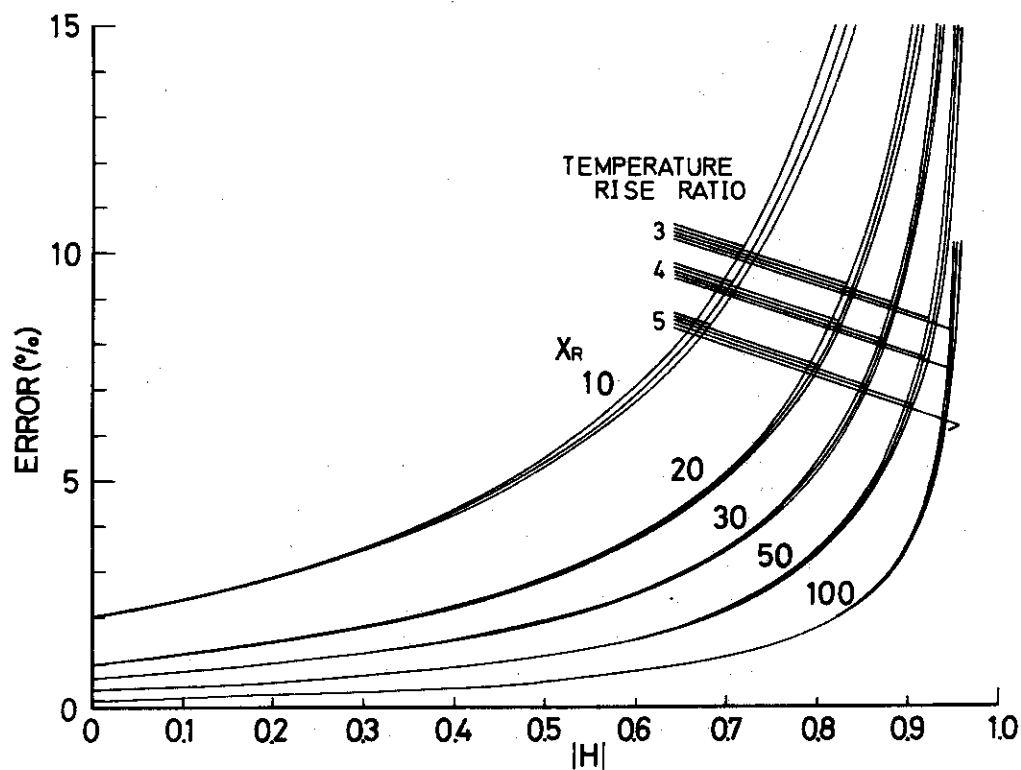


Fig. 11 Effect of the temperature rise ratio (3,4,5) on the relation of error vs. $|H|$ ($K=100$).

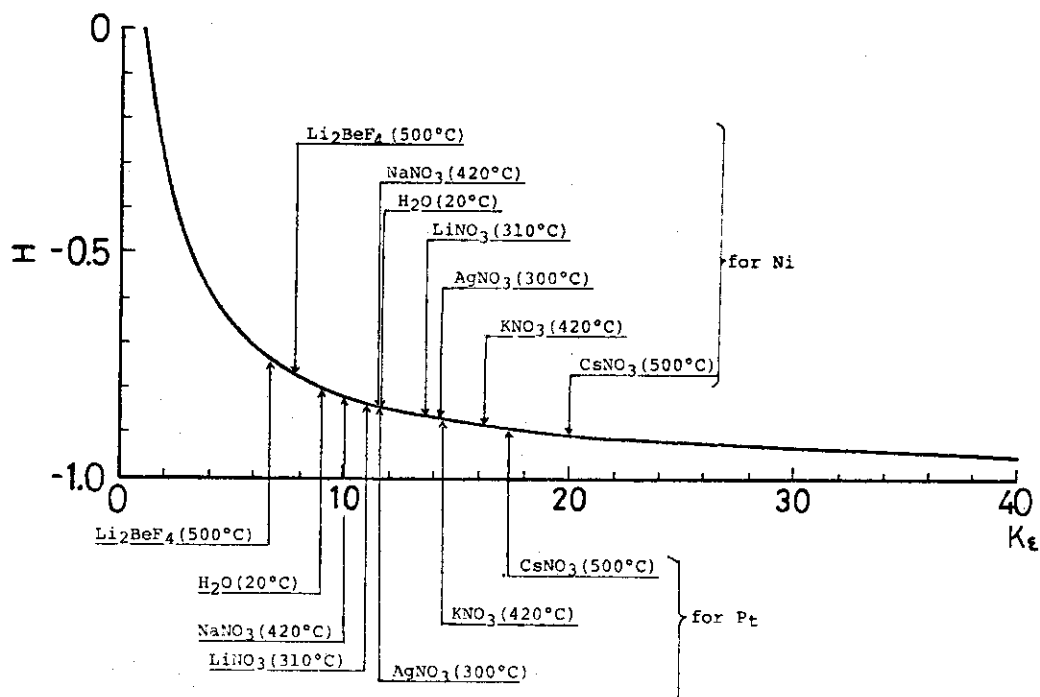


Fig. 12 Values of the parameter H of some molten salts and H_2O for Ni and for Pt. The values are plotted on a theoretical curve of H vs. K_E . $K_E = (\lambda_1 C_{p1} \rho_1 / \lambda_2 C_{p2} \rho_2)^{1/2}$, $H = (1 - K_E / (1 + K_E))$.

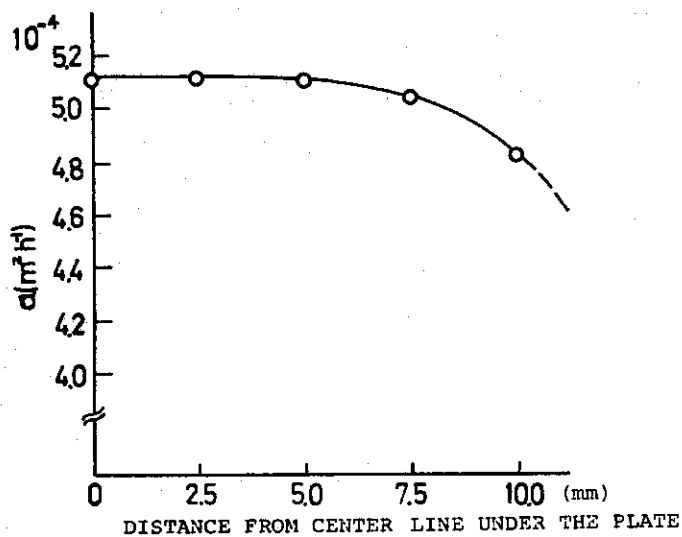


Fig. 13 Plot of the thermal diffusivities of H_2O (20°C) measured at the points from center line and parallel ($X_R=30$) to the Ni alloy heater plate ($32 \times 32 \times 0.1 \text{ mm}$). The heater plate is surrounded with Beryllia skirt.

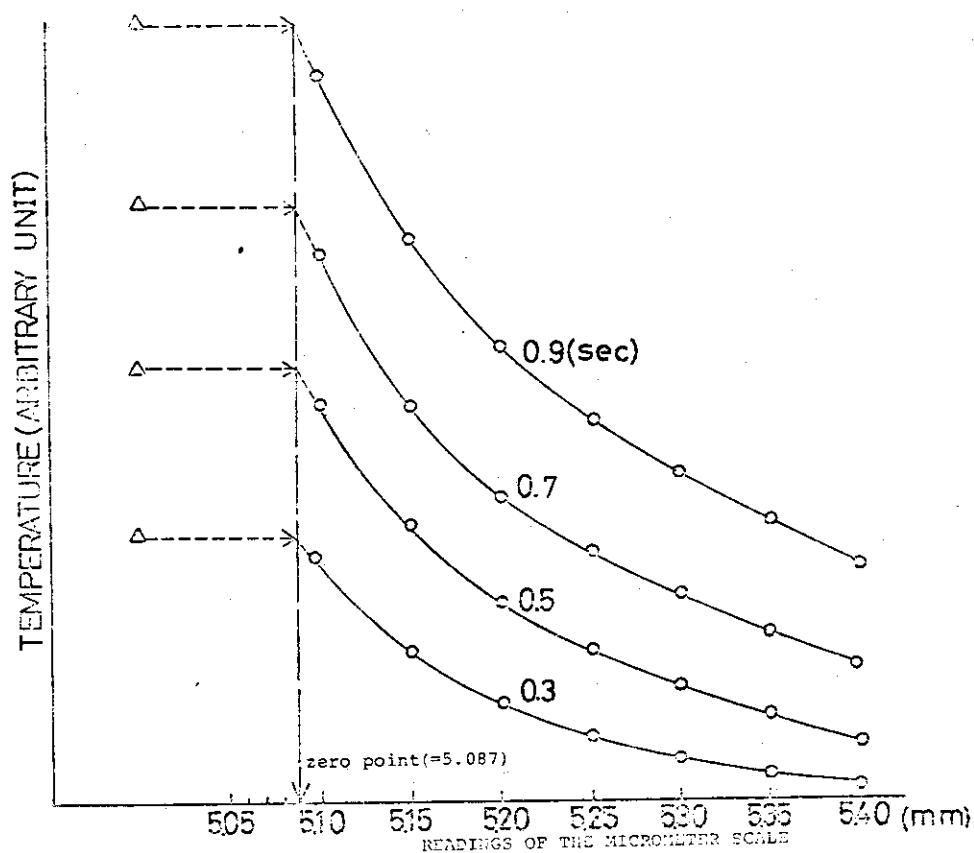


Fig. 14 A method to determine the position of zero point of the sheathed thermocouple. The cross point of two temperature curves of the liquid \circ and the heater plate Δ corresponds to the zero point.

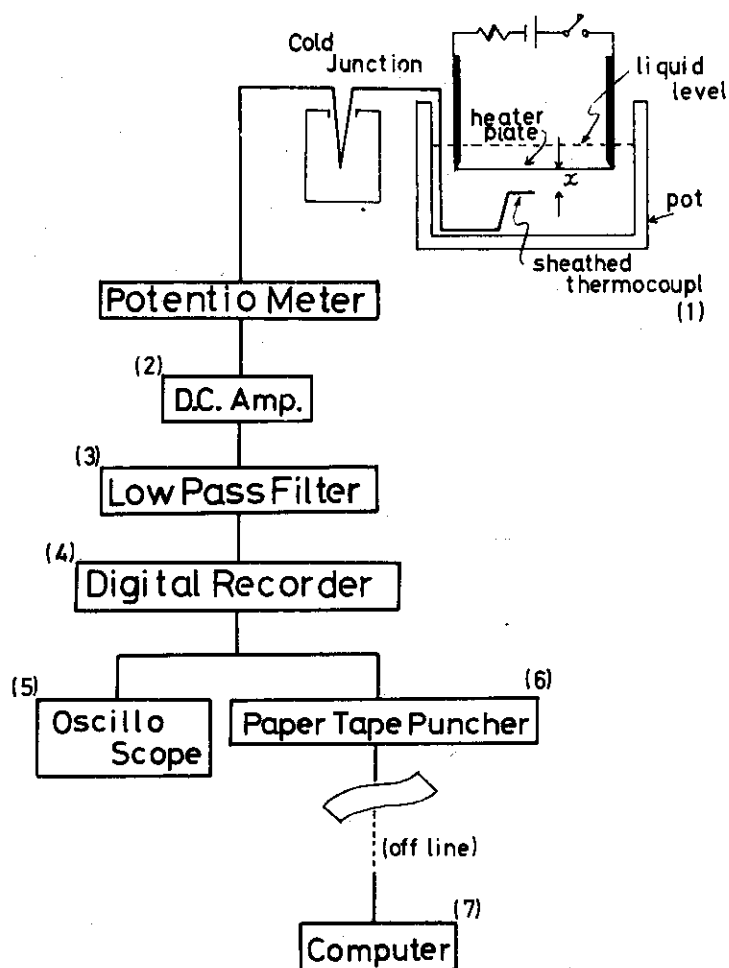


Fig. 15 Schematic diagram of the measuring system.

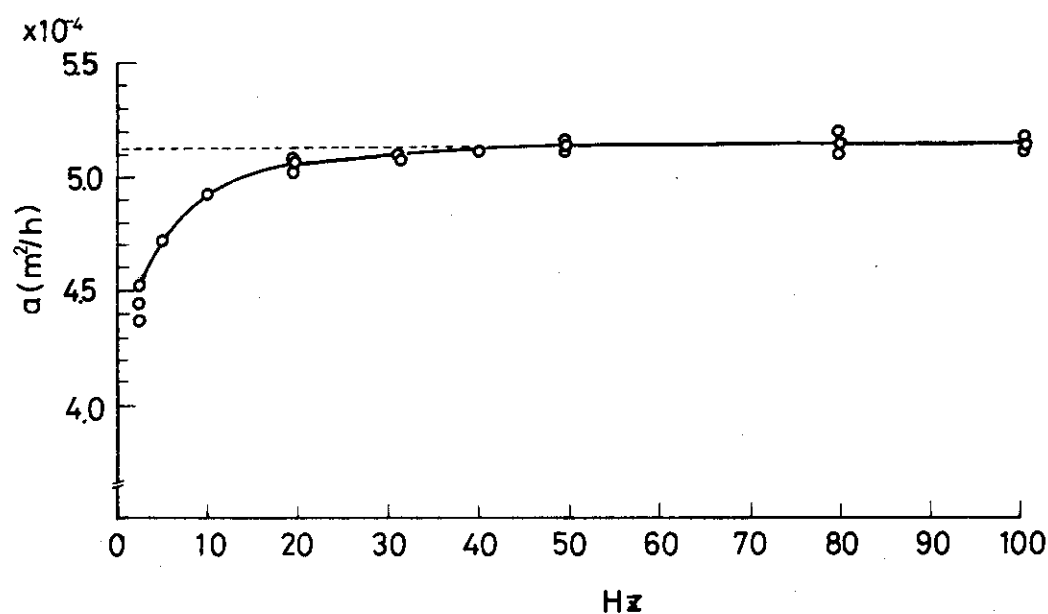


Fig. 16 Effect of the cutoff frequency of low pass filter (42db/oct decrease from cutoff frequency).
Sample liquid is $\text{H}_2\text{O}(20^\circ\text{C})$.

- 1 - heater plate (Ni alloy, 32x32x0.1mm).
- 2 - heater plate holder.
- 3 - Beryllia skirt.
- 4 - half-cylindrical shell electrodes.
- 5 - Inconel sheathed Chromel-Alumel thermocouple (0.25mm diameter)
- 6 - transparent quartz pot.
- 7 - quartz center pillar.
- 8 - micrometer
- 9 - radiation shield plate.
- 10 - outer heater furnace.

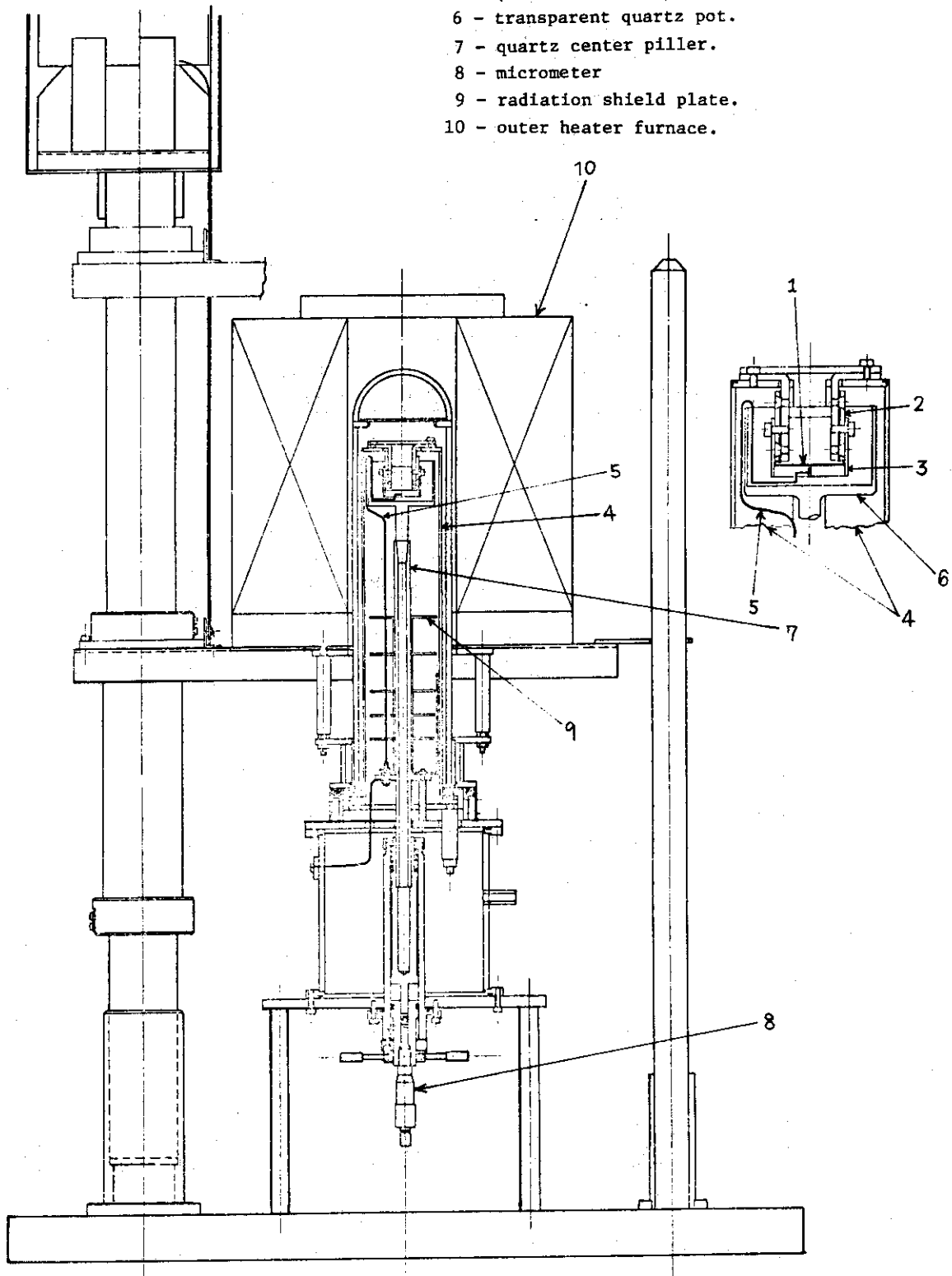


Fig. 17 Cross sectional view of the apparatus.

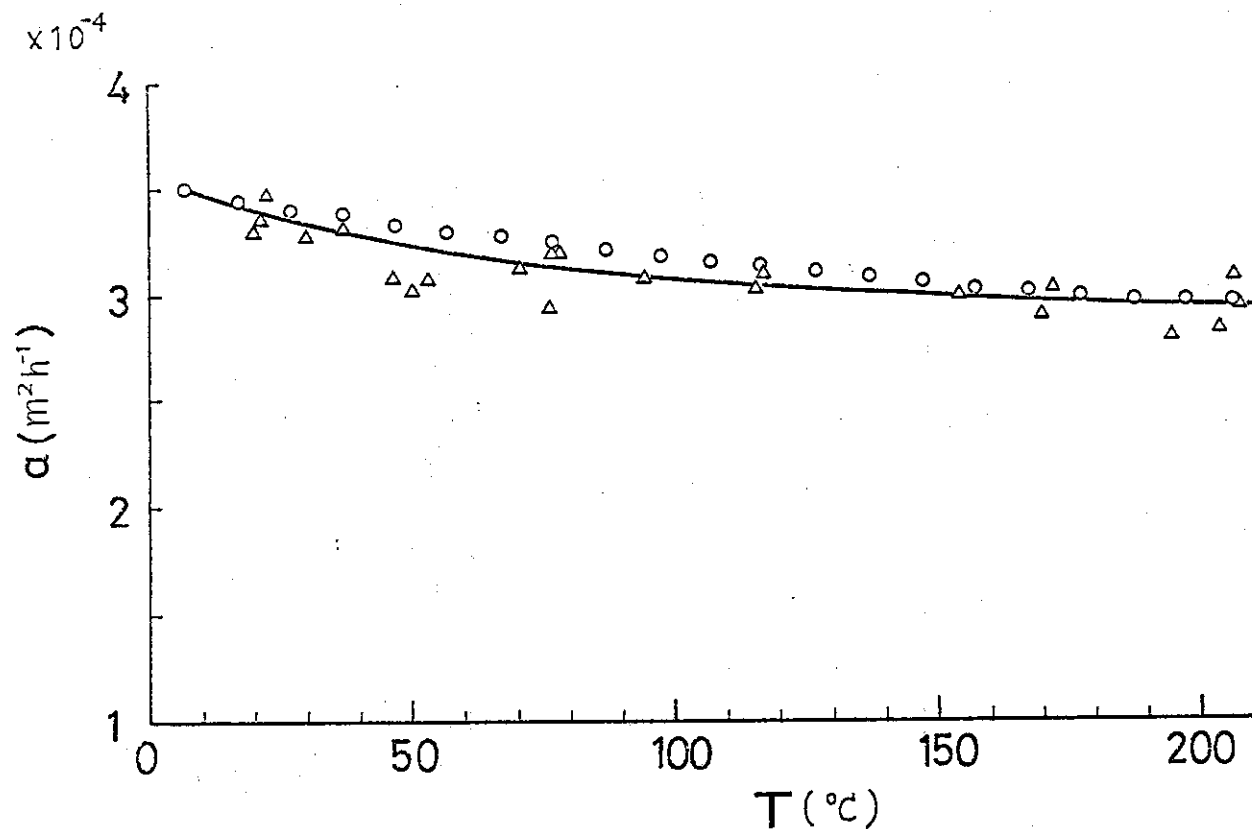


Fig. 18 Thermal diffusivity of glycerine. Δ present measurements; \circ converted from published data⁽⁴⁾

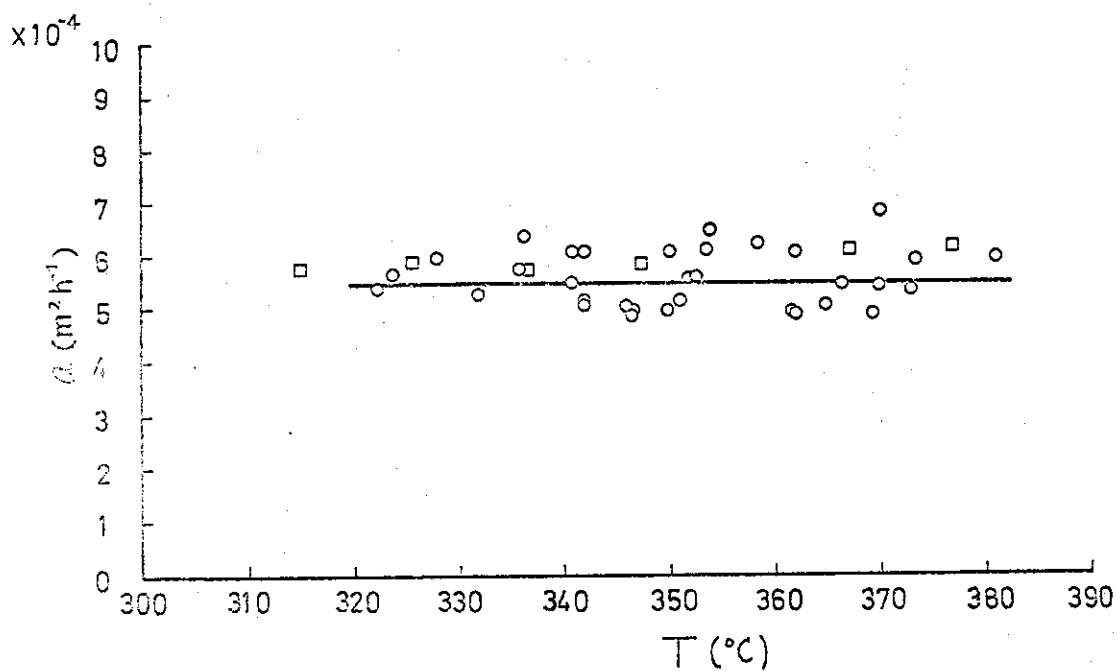


Fig. 19 Thermal diffusivity of molten NaNO_3 . \circ present measurements; \square published data⁽²⁾

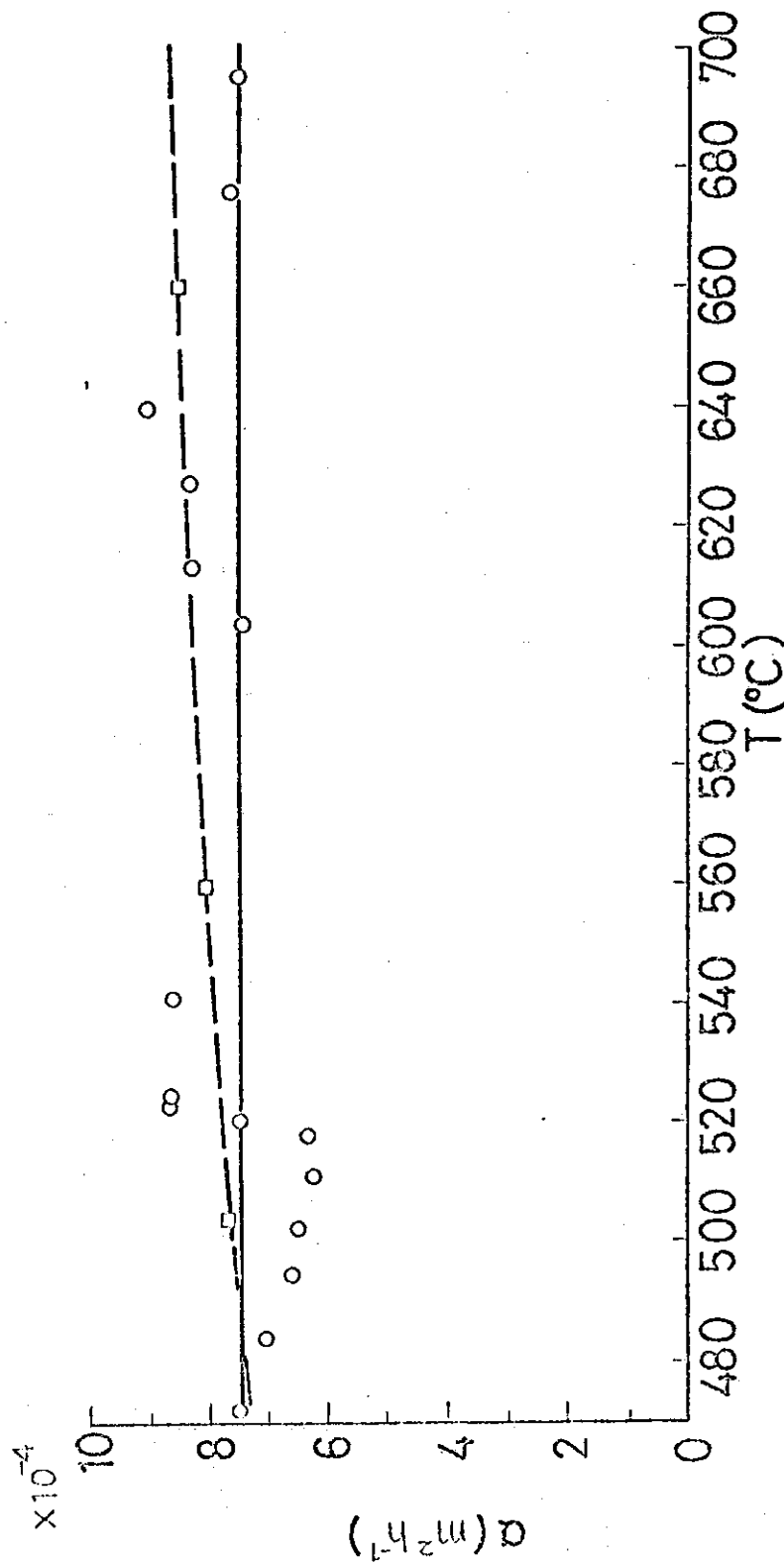


Fig. 20 Thermal diffusivity of molten Li_2BeF_4 .
 present measurements;
 converted from published data (5).